Deglacial Heat Uptake by the Southern Ocean and Rapid Northward Redistribution via Antarctic Intermediate Water

D.-W. Poggemann[1], D. Nürnberg[1†], E. C. Hathorne[1], M. Frank[1], W. Rath[1], S. Reißig[1], A. Bahr[2]

[1]GEOMAR Helmholtz Centre for Ocean Research Kiel, D-24148 Kiel, Germany.

[2]Heidelberg University, Institute of Earth Science, D-69120 Heidelberg, Germany.

Corresponding author: Dirk Nürnberg (dnuernberg@geomar.de)

† GEOMAR Helmholtz Centre for Ocean Research Kiel, D-24148 Kiel, Germany.

Key Points:

- Deglacial Mg/Ca-based intermediate water temperature changes in the tropical W-Atlantic.
- Prominent AAIW heat supply to the tropical Atlantic during AMOC perturbations after a detour via the Southern Ocean.
- Heat export via AAIW may have dampened deglacial southern hemisphere warming..

This article has been accepted for publication and undergone full peer review but has not been through the copyediting, typesetting, pagination and proofreading process which may lead to differences between this version and the Version of Record. Please cite this article as doi: 10.1029/2017PA003284

Abstract

Antarctic Intermediate Water (AAIW) is an important conduit for nutrients to reach the nutrient-poor low-latitude ocean areas. In the Atlantic, it forms part of the return path of the Atlantic Meridional Overturning Circulation (AMOC). Despite the importance of AAIW, little is known about variations in its composition and signature during the prominent AMOC and climate changes of the last deglaciation. Here, we reconstruct benthic foraminiferal Mg/Ca-based intermediate water temperatures ($IWT_{Mg/Ca}$) and intermediate water neodymium (Nd) isotope compositions at sub-millennial resolution from unique sediment cores located at the northern tip of modern AAIW extent in the tropical W-Atlantic (850 and 1018 m water depth). Our data indicate a pronounced warming of AAIW in the tropical W-Atlantic during Heinrich Stadial 1 (HS1) and the Younger Dryas (YD). We argue that these warming events were induced by major AMOC perturbations resulting in the pronounced accumulation of heat in the surface Southern Ocean. Combined with published results, our data suggest the subsequent uptake of Southern Ocean heat by AAIW and its rapid northward transfer to the tropical W-Atlantic. Hence, the rapid deglacial northern climate perturbations directly controlled the AAIW heat budget in the tropical W-Atlantic after a detour *via* the Southern Ocean. We speculate that the ocean heat redistribution *via* AAIW effectively dampened Southern Hemisphere warming during the deglaciation and may therefore have been a crucial player in the climate seesaw mechanisms between the two hemispheres.

1 Introduction

The role of AAIW in rapid climate changes resulting from major AMOC reorganisations is poorly constrained and interpretations of datasets are controversial (e.g. Came et al., 2008; Pahnke et al., 2008; Sotor and Lund, 2011; Xie et al., 2012; Huang et al., 2014; Freeman et al., 2015; Poggemann et al., 2017; Gu et al., 2017; Valley et al., 2017). The pronounced cold events of the last deglaciation HS1 (18 - 14.6 ka BP; Barker et al., 2009) and the YD (12.8 - 11.5 ka BP; Barker et al., 2009) were characterized by rapid cooling of the northern hemisphere (e.g. NGRIP Dating Group, 2006) and synchronous southern hemisphere warming (e.g. Stenni, 2006), while the AMOC weakened or even collapsed (e.g. McManus et al., 2004; Böhm et al., 2015). Previous studies argued for the reduced northward advection of AAIW during HS1 and the YD, and the replacement of AAIW by northern-sourced water masses (Came et al., 2008; Xie et al., 2012). Other studies, in contrast, either suggested an increased northward advection of AAIW during these periods of time (Zahn & Stüber, 2002; Pahnke et al., 2008) or only minor changes in its distribution (Huang et al., 2014; Howe et al., 2016).

Today, the overturning in the Atlantic is mainly driven by the formation of North Atlantic Deep Water (NADW) in the N-Atlantic, which in turn receives contributions from AAIW and warm and saline tropical waters (e.g. Talley, 2013). During the Last Glacial Maximum (LGM), in contrast, the AMOC was likely split into two separate overturning cells (e.g. Ferrari et al., 2014). During the transition from the LGM to the Holocene, when the AMOC experienced major changes (e.g. McManus et al., 2004; Böhm et al., 2015), these overturning cells presumably reconnected (Poggemann et al., 2017). Due to these AMOC perturbations and the related reduction in northward heat transport, modelling and proxy data suggested heat accumulation in the tropical Atlantic and in the Southern Ocean (e.g. Rühlemann et al., 1999; Vellinga & Wood, 2002; Toggweiler & Lea, 2010; Schmidt et al., 2012). Southern

Ocean sea-surface temperature (SST) reconstructions for the last deglaciation exhibit major warming during northern hemisphere cold events pointing to a seesaw mechanism between the high-latitude ocean areas (e.g. Kaiser et al., 2005; Calvo et al., 2007; Lamy et al., 2007; Stenni et al., 2011; Landais et al., 2015). Synchronous upwelling of old, nutrient-rich, and carbon-enriched water masses in the Southern Ocean and the concomitant release of CO_2 to the atmosphere accompanied northern hemisphere cold events (e.g. Anderson et al., 2009; Burke & Robinson, 2012). These processes may have triggered ventilation and nutrient enrichment of AAIW (Burke & Robinson, 2012; Poggemann et al., 2017).

Despite the absence of suitable sediment records and the lack of direct temperature reconstructions from intermediate water depths, previous studies argued for the transfer of the Southern Ocean surface temperature signature *via* intermediate waters into the (sub)tropics (e.g. Kiefer et al., 2006; Naidu & Govil, 2010; Romahn et al., 2014). In particular during deglacial AMOC perturbations, atmospheric changes in temperature and wind strength may have affected the composition of AAIW and its geochemical signatures, which then would have been transferred from the (sub)Antarctic regions to the tropics (e.g. Lynch-Stieglitz et al., 1994; Ninnemann & Charles, 1997; Spero & Lea, 2002; Bostock et al., 2004). Direct evidence for the postulated warming from intermediate water records is, however, lacking and the processes controlling low latitude intermediate temperature evolution remain unclear. Here, we present the first high resolution deglacial AAIW temperature reconstruction in the tropical W-Atlantic based on benthic foraminiferal Mg/Ca. The foraminiferal specimens were selected from the unique sediment core M78/1-235-1 from Tobago Basin (tropical W-Atlantic) from 852 m water depths, which is in the core of modern AAIW. Combined with reconstructed intermediate water neodymium isotope (εNd) signatures obtained from uncleaned planktonic foraminifera (sediment core M78/1-222-9, S-Caribbean), we are able to reconstruct the past variability of heat transfer from the Southern Ocean to the tropical

Atlantic *via* AAIW and its possible relationship to changes in Atlantic water mass mixing and circulation.

2 Materials and Methods

2.1 Sediment cores and foraminifera selected for analyses

The Mg/Ca-ratio of benthic foraminiferal tests is a well-established proxy for bottom water temperature reconstructions (e.g. Bryan & Marchitto, 2008; Elderfield et al., 2010). We analyzed Mg/Ca of the endobenthic foraminiferal species *Uvigerina* spp. selected from sediment core M78/1-235-1 (11°36.53'N, 60°57.86'W; termed Core 235 in the following). The core was retrieved from the Tobago Basin (SE-Caribbean) from 852 m water depth, which is within the core of modern AAIW (Fig. 1). *Uvigerina* spp. is not influenced by carbonate ion effects at intermediate water depth, which makes $Mg/Ca_{Uvigerina}$ a suitable proxy to estimate past changes in $IWT_{Mg/Ca}$ (Elderfield et al., 2010; Elmore et al., 2015). We use the established age model of Core 235 (Poggemann et al., 2017), which was generated by linear interpolation between 9 $AMS^{14}C$ dates.

We further determined the εNd signatures of uncleaned mixed planktonic foraminifera to reconstruct changes in the mixing of the prevailing intermediate water masses. Previous studies have proven that authigenic coatings of uncleaned planktonic foraminiferal tests reliably record past bottom water εNd signatures (e.g. Roberts et al., 2010; Piotrowski et al., 2012; Huang et al., 2014). Due to the lack of available sample material in Core 235, the εNd signatures were extracted from nearby sediment core M78/1-222-9 (12°1.49'N, 64°28.50'W, 1018 m; termed Core 222 in the following). Core 222 was retrieved from the southern Caribbean Sea north of Blanquilla Island and located at the lower boundary of modern AAIW (Fig. 1). The age model for Core 222 is based on linear interpolation between 4 $AMS^{14}C$ dates (Table S1) and supported by oxygen isotope stratigraphy (see supporting information;

Fig. S1). Due to the low abundance of benthic foraminifera in Core 222, we were not able to accomplish Mg/Ca-based bottom water reconstructions for this core. A detailed discussion of the methodology can be found in the supporting information.

All sediment samples were freeze dried, wet sieved, and size fractionated. For Mg/Ca-ratios, ~30 benthic foraminiferal tests of *Uvigerina* spp. from the 315 - 400 µm size fraction were selected. For εNd analyses, >45 mg of mixed planktonic foraminiferal shells from the >250 µm size fraction were picked.

2.2 Mg/Ca analyses

For Mg/Ca analyses, the foraminiferal samples were cleaned oxidatively and reductively following established protocols (e.g. Barker et al., 2003) and measured on an Varian 720-ES Axial ICP-OES and Agilent 7500ce ICP-MS at GEOMAR (supporting information, dataset S1). The Mg/Ca measurements were drift-corrected and standardized to the internal consistency ECRM752-1 standard (3.761 mmol/mol Mg/Ca; Greaves et al., 2008). The external reproducibility for the ECRM standard is ±0.1 mmol/mol for Mg/Ca (standard deviation 2σ). Replicate measurements run during different sessions reveal a reproducibility of max. ~0.24 mmol/mol (2σ).

The calculated Mg/Ca-ratios of the infaunal *Uvigerina* spp. were converted to absolute (intermediate water) temperatures ($IWT_{Mg/Ca}$) using the established calibrations of Elderfield et al. (2010) and Martin et al. (2002). The error (2σ) of the calculated $IWT_{Mg/Ca}$ is ~1°C. The well-elaborated Elderfield et al. (2010) based on core-top *Uvigerina* spp. suggests a linear relationship between Mg/Ca and bottom water temperature (Mg/Ca = 1 + 0.1 T). Instead, Martin et al. (2002) corrected downcore *Uvigerina* spp. Mg/Ca to match with Mg/Ca of *C. wuellerstorfi* for which they had derived an exponential temperature sensitivity (Mg/Ca = 0.76 * exp(0.15 T). Both calibrations provide late Holocene (last 5 ka) $IWT_{Mg/Ca}$ of ~4 $\pm$ 1°C, which are close although lower by ~1°C to the modern IWT (~4.5 -5.5°C) at the

location of Core 235 (Fig. 2; Fig. S2). Across the deglaciation, the $IWT_{Mg/Ca}$ amplitude variations differ, with the Elderfield et al. (2010) calibration providing a larger $IWT_{Mg/Ca}$ amplitude than the exponential Martin et al. (2002) equation (maximum downcore range of ~9°C compared to ~4°C). As both approaches appear justified, we decided to present the $IWT_{Mg/Ca}$ reconstructions obtained from both calibrations as our best minimum to maximum estimates of deglacial IWT variability. All other calibrations available for *Uvigerina* spp. yield $IWT_{Mg/Ca}$ clearly warmer than the modern IWTs, provide extremely large downcore $IWT_{Mg/Ca}$-amplitudes, and were thus considered inappropriate. Further details are given in the supporting information and Fig. S2.

There is no evidence for sample contamination by clay minerals and/or diagenetic coatings assessed from Al/Ca, Mn/Ca and Fe/Ca ratios, ruling out any falsifying effect on the reconstructed $IWT_{Mg/Ca}$. A detailed discussion can be found in the supporting information (Figs. S3, S4; Barker et al., 2003; Them et al., 2015; Roberts et al., 2016). A small number of single data points yielded unrealistically high/low values compared with neighboring data. By applying the Grubbs test (Grubbs, 1950), a total of 16 Mg/Ca data points were consequently defined as outliers and removed from the record of Core 235. Further details are given in the supporting information (Fig. S5; Grubbs, 1950, 1969). $Cd/Ca_{Uvigerina}$ data from the same samples were already presented in Poggemann et al. (2017) (Fig. 4).

2.3 Nd isotope measurements

Preparation for Nd isotope analyses followed the protocols of Roberts et al. (2010; 2012) and Piotrowski et al. (2012). Briefly, the crushed mixed planktonic foraminiferal samples were inspected under a binocular microscope and any visible detritus removed before being physically cleaned by repeated rinses with <18 MOhm water and ethanol while being placed in an ultrasonic bath. Once visibly clean, the calcite was dissolved carefully in ~0.35 M acetic acid to avoid leaching of any minor amounts of detrital material remaining, then centrifuged

and transferred into Teflon vials. Chemical purification of Nd from the sample solutions was performed with established methods (e.g. Barrat et al., 1996; Le Fèvre & Pin, 2005; Roberts et al., 2012; Osborne et al., 2014). The Nd isotope data were measured mainly on a Thermo Fisher Scientific Neptune MC-ICP-MS at the University of Oldenburg. Only 4 samples were measured on a Nu Plasma Multi Collector ICP-MS at GEOMAR (c.f. Table. XX PANGAEA). All $^{143}Nd/^{144}Nd$ results were normalized to the established value for the JNdi-1 standard of 0.512115 (Tanaka et al., 2000). The 2σ external reproducibility of the Nd isotope measurements based on repeated standard measurements at different concentrations ranged between 0.1 and 0.5 εNd units depending on sample size and instrument used (Nu Plasma MC-ICP-MS: 0.3 εNd units; Neptune MC-ICP-MS: 0.1-0-5 εNd units).

3 Results

Dependant on the Mg/Ca *vs.* temperature calibration applied (Martin et al., 2002; Elderfield et al., 2010), the reconstructed $IWT_{Mg/Ca}$ differ largely (Fig. 2). In the low-temperature range <5°C, both calibrations provide rather resembling $IWT_{Mg/Ca}$ estimates deviating by only half a degree, but the linear format of the Elderfield et al. (2010) equation most likely overestimates the $IWT_{Mg/Ca}$ in the high-temperature range (>5°C). Peak $IWT_{Mg/Ca}$ calculated by the Elderfield et al. (2010) equation are by up to ~4°C warmer than those from the Martin et al. (2002) equation. The resulting relative changes of $IWT_{Mg/Ca}$, however, are considered credible and are applied for interpretation.

During full glacial times (~24 - 18 ka BP), the $IWT_{Mg/Ca}$ at the location of Core 235 was in the range of ~3.8 $\pm$ 0.8°C, depending on the Mg/Ca *vs.* temperature calibration applied (Fig. 2). This is only ~1°C lower than modern AAIW annual temperatures of 4.5 - 5.5°C (WOA2013; Boyer et al., 2013). During HS1 the $IWT_{Mg/Ca}$ rapidly rose by ~3 - 7°C to maximum values of ~6.7 - 10.9°C at the end of HS1 (~15.5 ka BP). Afterwards, a marked drop in $IWT_{Mg/Ca}$ by ~4 - 7°C is apparent, ending at ~14.8 ka BP at $IWT_{Mg/Ca}$ of ~2.8 - 3.5°C

close to those of full glacial conditions (Fig. 2). The $IWT_{Mg/Ca}$ subsequently reached a maximum of ~4.8 - 5.8°C at ~14.5 - 14.2 ka BP, at the beginning of the Antarctic Cold Reversal (ACR, ~14.5 - 12.8 ka BP, Anderson et al., 2009). This increase was again followed by a rapid drop to on average 4.5 - 5°C close to modern-like values (~14 - 13 ka BP). The YD was characterized by gradually increasing $IWT_{Mg/Ca}$ by ~2 - 3°C and reached mean values of ~5 - 6°C (max. 9°C) during the early Holocene (~11 - 10 ka BP). The remaining Holocene period was characterized by a gradual decline in $IWT_{Mg/Ca}$ of overall ~2°C finally reaching values of ~4°C (Fig. 2), which was slightly cooler than the modern IWT at the core location (WOA2013; Boyer et al., 2013).

In order to further investigate intermediate water dynamics in the tropical W-Atlantic, we compared the Core 235 $IWT_{Mg/Ca}$ record to the εNd record of adjacent Core 222. The reconstructed intermediate water εNd pattern clearly differs from that of the $IWT_{Mg/Ca}$ record (Fig. 2). The εNd data show a gradual and continuous decline from more radiogenic values of ~-9.8 on average during full glacial times (~24 - 18 ka BP) to less radiogenic values of ~-11.5 during the late Holocene (last ~4 kyr). During the deglaciation, in particular during late HS1 to shortly after the YD, when $IWT_{Mg/Ca}$ were characterized by prominent variations, the εNd signal remained essentially stable at ~-11. These Nd isotope data are consistent with bottom water data obtained on measurements of fish debris from a nearby core at similar water depths (Xie et al., 2014; Fig. 3), for which it was shown that reliable bottom water εNd signatures were extracted given the absence of any correlation to the significantly less radiogenic detrital fraction.

4 Discussion

4.1 Intermediate depth warming in the tropical W-Atlantic: replacement of water mass vs. signature change

The reconstructed $IWT_{Mg/Ca}$ record reveals prominent warming phases during HS1, synchronous to the early ACR, and from the YD to the early Holocene, which documents enhanced heat transfer into the intermediate tropical W-Atlantic (Fig. 3). These temperature peaks may be explained by three possible scenarios, a replacement of AAIW with a warmer water mass, a local warming from above, or a warming of AAIW itself. We find our data to be most supportive of the third scenario.

The first scenario implies that cold nutrient-rich AAIW was replaced by or at least experienced major admixture of a warmer and nutrient-depleted northern-sourced water mass during short deglacial time intervals. Such a replacement of AAIW by or a major admixture of northern-sourced water masses from overlying water depths would also have to be reflected by pronounced changes in a variety of proxies (e.g. εNd, nutrient and $\delta^{13}C$ reconstructions). Previously published benthic (*Uvigerina* spp.) $\delta^{13}C$ and Cd_w reconstructions obtained from the same Core 235 foraminiferal sample material (Fig. 4) clearly argue for enhanced nutrient supply to the tropical W-Atlantic at intermediate water depth during late HS1, as well as during and shortly after the YD (Poggemann et al., 2017). These short-term nutrient injections, however, were suggested to be mainly due to changes in the nutrient budget of water masses forming AAIW in the Southern Ocean by upwelling processes. Poggemann et al. (2017) argued in detail that the nutrient injections were caused by the replacement of AAIW or enhanced mixing with deeper Circumpolar Deep Water (CPDW) (Fig. 4).

The comparison between intermediate water nutrient conditions in the tropical W-Atlantic (Poggemann et al., 2017) and Florida Straits (Came et al., 2008; Valley et al., 2017) across

the deglaciation highlights a rather complicated situation at intermediate depths, which is not solely related to AAIW dynamics (see supporting information; Came et al., 2008; Poggemann et al., 2017; Valley et al.; 2017). Today, driven by the Caribbean Current, AAIW flows across Yucatan Straits into the Gulf of Mexico, where it disperses *via* anticyclonic rings (eddies) that are shed by the Loop Current. During its trajectory, the AAIW increases in salinity, while its thickness is reduced considerably. In the Gulf of Mexico, the depth of occurrence of the AAIW remnant varies (620-900 m), depending on the presence and interaction of the eddies (Vidal et al., 1994), and AAIW remnants finally lose their AAIW signature. These features are likely responsible for the differences between the two locations at intermediate depth levels in the tropical W-Atlantic and the Florida Straits.

The second scenario involves increasing IWTs by local warming from above. Weldeab et al. (2016) observed an accumulation of heat in the mid-depth (~1300 m water depth) equatorial E-Atlantic during HS1 and the YD and explained it by 1-D-downward (vertical) diffusion processes at times of AMOC perturbations. Schmidt et al. (2017) and Parker et al. (2015), who presented subsurface-temperature (~200-300 m water depth) records from both, the equatorial W and E-Atlantic, instead, argued that vertical diffusion of ocean heat from the surface to the subsurface (and even deeper) is much too slow to explain the abrupt (millennial-scale) warming processes of up to 5°C during both HS1 and the YD.

Following the reasoning of Schmidt et al. (2017), we rule out local warming from above as the mechanism for increased IWTs at the location of Core 235 and note that the comparison of our reconstructed $IWT_{Mg/Ca}$ to subsurface temperatures ($subSST_{Mg/Ca}$, ~400 m water depth) obtained from a nearby sediment core VM12-107 from the Bonaire Basin (Schmidt et al., 2012; Fig. 1) shows markedly different patterns of warming during the deglaciation (Fig. 3). This implies that intermediate and subsurface-water dynamics were decoupled in the study area and that vertical diffusion of heat from the surface cannot have reached depths of 800 m.

We also note that additional vertical diffusional heat exchange between the surface and the intermediate-depth ocean (~800 m water depth) would afford a reduced water column stratification, which cannot have occurred without major water mass mixing. Mixing processes, however, would be distinctly reflected by the alteration of the water-mass composition and should therefore be seen in other proxies such as Cd_w and εNd, which is not the case. These authors favor a scenario that involves horizontal propagation of ocean heat at subsurface depths from the extratropical North Atlantic to the equatorial region. In this respect, the expansion of Salinity Maximum Water of the N-Atlantic Subtropical Gyre in response to a rapidly changing AMOC would play a leading role for equatorial Atlantic subsurface warming.

We therefore argue that the most likely scenario for the $IWT_{Mg/Ca}$ warming involves a significant change in AAIW properties in its formation areas in the Southern Ocean themselves and a subsequent northward transport of the modified thermal AAIW signature into the tropical W-Atlantic. In support of this, our previously published Cd_w and $\delta^{13}C$ records (based on *Uvigerina* spp.) from Core 235 documented major increases in the nutrient content of AAIW during northern hemisphere cold events, initiated by changes in Southern Ocean upwelling (Poggemann et al., 2017; Fig. 4).

We further test the compatibility of the postulated changes in water-mass density during times of rapid "mid-depth warming" with an un-changed (modern) location of AAIW in the water column by estimating static stability (details are given in the supporting information; Fig. S6). The results indicate that a selective increase of deglacial AAIW temperatures by 5°C while SST remained low does not result in hydrographic instability (always positive values in Fig. S6E), even in this extreme scenario. It is interesting to note that these calculations suggest that AAIW may have slightly shoaled as a result of the warming (values near zero in Fig. S6E), which is consistent with the modelling results of Gu et al. (2017).

The AAIW εNd reconstruction obtained from tropical W-Atlantic Core 222 (Fig. 2) allows the distinction between the admixed water masses and supports the postulated mechanisms. Today, the εNd signature for NADW is -13.5 as a consequence of weathering inputs of old continental material surrounding the N-Atlantic, in particular the Labrador Sea (Piepgras & Wasserburg, 1987). In contrast, Pacific subsurface water masses are characterized by more radiogenic signatures of -2 to -4 originating from weathering of young volcanic rocks surrounding the Pacific (Piepgras & Wasserburg, 1980; Piepgras & Jacobsen, 1988). In the Southern Ocean, the formation area of AAIW, water masses are a mixture of Pacific and Atlantic water masses and are therefore characterized by intermediate εNd signatures of -6.2 to -9.2 (Jeandel, 1993). Along its northward advection in the Atlantic, the modern AAIW εNd signature of ~-8.4 (Stichel et al., 2012; Molina-Kescher et al., 2014) is modified by both, water mass mixing (Jeandel, 1993) and, to some extent, through external inputs (e.g. release from and exchange with sedimentary Nd), which results in a less radiogenic signature of ~-10.5 to -11 by the time AAIW reaches the tropical W-Atlantic (Huang et al., 2014; Osborne et al., 2014). New detrital εNd data from the Demerara Rise confirm the presence of more unradiogenic sediments in the region (Howe et al., 2016). In contrast to modern NADW, the εNd signature of Glacial North Atlantic Intermediate Water (GNAIW), which replaced NADW during glacial times (Marchitto & Broecker, 2006) has been inferred to be similarly unradiogenic as today's NADW (van de Flierdt et al., 2006; Foster et al., 2007; van de Flierdt et al., 2016), but according to other records may have been as radiogenic as -10 (Gutjahr et al., 2008).

A recent study directly modelling changes in the εNd of AAIW in the study region during the deglaciation (Gu et al., 2017) reproduces an existing εNd reconstruction from the Bonaire Basin (Core VM12-107, Xie et al., 2014) and our new εNd record from Tobago Basin Core 235 (Figs. 1, 3). The variability of these data was previously ascribed to a gradual change

from GNAIW-dominated admixture during the LGM to NADW dominated admixture during the Holocene, but Gu et al. (2017) suggested a significant influence from the enhanced upwelling of radiogenic Caribbean Deep Waters during the LGM, which then declined during the deglaciation. However, comparison of the results from the control run with the modern isotopic composition in the region suggests that the model overestimates the influence of radiogenic Caribbean Deep Waters (see their Fig. 2). Additionally, the model of Gu et al. (2017) produced a considerably weaker present-day AAIW northward penetration compared to observations as exhibited by the salinity section from the control run (see their Fig. 2). Slight differences between the new εNd record presented here and that of Xie et al. (2014) (Fig. 3) are best explained by the locations of the cores being differently affected by weathering inputs from highly radiogenic volcanic rocks or unradiogenic sediments altering the water mass signature locally (Osborne et al., 2014). Both, the overall consistency of the S-Caribbean εNd records and the lack of perturbations during the deglacial HS1 and YD cool events, which were observed at other locations (e.g. Tobago Basin Core MD99-2198, Pahnke et al., 2008; Demarara Rise cores KNR197-3-25GGC, KNR197-3-46CDH, KNR197-3-9GGC, Huang et al., 2014; Brazil margin cores GeoB2107-3, KNR159-5-36GGC, and GeoB2104-3, Pahnke et al., 2008 and Howe et al., 2016; Fig. 1), suggests that the local overprinting of bottom seawater was minimal, while the modification of AAIW from -8.4 in the Southern Ocean and S-Atlantic to values of -10.5 to -11 observed in the tropical W-Atlantic and Caribbean today persisted throughout the last 24 kyrs. Combined with the evidence from previously published Cd_w and $\delta^{13}C$ reconstructions from Tobago Basin Core 235 (Poggemann et al., 2017), we interpret the εNd record of both S-Caribbean cores (Core 235 and Core VM12-107; Fig. 3) in terms of a gradual change in the εNd signature of AAIW caused by the combination of a continuous supply of AAIW from the Southern Ocean, supported by the results of Howe et al. (2016) from the Brazil margin, and a decreasing

admixture of radiogenic deep waters from the Caribbean between the LGM and the Holocene (Gu et al., 2017).

Nutrient and ventilation reconstructions from the tropical W-Atlantic may suggest a change in the composition of water masses forming AAIW due to Southern Ocean upwelling changes (Poggemann et al., 2017). However, the similarity of the εNd signatures of GNAIW and CPDW during the last glacial (Gutjahr et al., 2008) and the alteration of the AAIW εNd signature *via* mixing on its pathway into the N-Atlantic mean that large changes in the εNd of AAIW are not to be expected (Xie et al., 2014). Assuming a more radiogenic εNd signature of GNAIW near -10 (Gutjahr et al., 2008), the glacial εNd values of ~-9.7 in both records are consistent with the notion of GNAIW being the main source water mass for AAIW during full glacial times (e.g. Ferrari et al., 2014; Poggemann et al., 2017), which is supported by the constant AAIW Nd isotope signatures in the western S-Atlantic published by Howe et al. (2016). During HS1 and the YD when NADW formation collapsed / weakened, the upwelling of nutrient-rich deep CPDW in the Southern Ocean, mainly feeding the AAIW, was enhanced (Anderson et al., 2009; Poggemann et al., 2017). In support of this, the εNd records from Tobago and Bonaire basins (Core 235, this study; Core VM12-107, Xie et al., 2014; Figs. 1, 3) show close to local modern AAIW values (~-10.4 to -11) arguing for a continuous supply of AAIW from the Southern Ocean during times of rapid northern hemisphere cold periods. Since the beginning of the Holocene, AAIW was fed by both, CPDW and NADW and the enhanced contribution of NADW most likely explains the less radiogenic values during the Holocene (~-11 to -12), consistent with Howe et al. (2016). Even so, the complex interplay of a still unidentified origin of the modification of AAIW to less radiogenic values between the Brazil margin (Howe et al., 2016) and the Caribbean (Huang et al., 2014; Osborne et al., 2014) and the variable admixture of more radiogenic Caribbean deep waters (Osborne et al., 2014; Gu et al., 2017) means that the Nd isotope

records cannot provide unambiguous or quantitative information on changes in the mixture of AAIW at its source region or its volume flow.

Nonetheless, based on the data of Howe et al. (2016) from the western S-Atlantic, the εNd data are consistent with a continuous deglacial supply of AAIW to the tropical W-Atlantic, serving as a persistent means of transport for variable nutrient and heat signatures introduced in the Southern Ocean. Irrespective of the strength of AAIW advection from the Southern Ocean, the published LGM and the Holocene Cd_w and $\delta^{13}C$ data from Tobago Basin Core 235 (Poggemann et al., 2017) are still consistent with the overall shift from GNAIW being the major contributor feeding into the AAIW during the LGM to CPDW and upper NADW being the main source waters during the Holocene, which is consistent with the circulation changes inferred by Ferrari et al. (2014).

4.2 The southern detour: Heat accumulation in the Southern Ocean due to AMOC perturbations triggered AAIW warming in the tropical W-Atlantic

At present, the surface-limb of the AMOC effectively transports oceanic heat into the N-Atlantic, thereby cooling the southern hemisphere (e.g. Crowley, 1992). During deglacial times of rapid northern hemisphere cooling, namely during HS1 and YD, major warming events in the southern hemisphere occurred, validating the seesaw pattern in ocean temperatures between the hemispheres (e.g. Broecker, 1998; Stocker, 1998; Kaiser et al., 2005; Calvo et al., 2007; Lamy et al., 2007; Toggweiler & Lea, 2010; Stenni et al., 2011; Landais et al., 2015). The observed intervals of heat accumulation in the southern hemisphere hence may have been caused by a weakened or collapsed AMOC (e.g. Denton et al., 2010). Due to the heat-storage capacity of the Southern Ocean, a ceased AMOC is suggested to result in Southern Ocean warming with a response time of ~1000 years (Stocker & Johnson, 2003; Hansen et al., 2016). Accordingly, the observed weakening/collapse of deep water formation in the N-Atlantic (McManus et al., 2004; Böhm et al., 2015) would have led to

reduced heat transfer from the southern hemisphere into the N-Atlantic and therefore should have increased SST in the Southern Ocean.

Southern Ocean sea-surface warming during AMOC perturbations is considered a prime reason for intermediate water warming in the tropical W-Atlantic (e.g. Stocker, 1998; Toggweiler & Lea, 2010; Stenni et al., 2011; Landais et al., 2015). Alkenone and foraminiferal $Mg/Ca_{G.bulloides}$-based SST data from off S-Australia (Core MD03-2611, ~36°S, Calvo et al., 2007) and Chatham Rise off New Zealand (Core MD97-2120, ~45°S, Pahnke et al., 2003) reveal a 2-step-warming pattern across the deglaciation with distinct warmings of ~3-5°C during HS1 and ~2-3°C during the YD, while during the ACR SSTs remained as high as during HS1 (Fig 3). In particular near the modern AAIW formation areas off S-Chile (Fig. 1), Lamy et al. (2007) also observed a deglacial 2-step-warming pattern with amplitude changes in their alkenone-based SST record (ODP Site 1233, ~41°S) similar to our tropical W-Atlantic intermediate depth record (Fig. 3). While the sea-surface warming in the Southern Ocean appears rather gradual and continuous without significant intermittent cooling periods, the tropical W-Atlantic $IWT_{Mg/Ca}$ reflects a deglacial sequence of rapid centennial-scale and large-amplitude (~3 - 4°C to max. ~7°C) warming (H1 into the early ACR, YD into the early Holocene) and cooling periods (late HS1 and late ACR). Nonetheless, both the rapidity of warming and its absolute amplitude were similar at both regions and water depths (Fig. 3). The temporal correspondance of the tropical W-Atlantic $IWT_{Mg/Ca}$ changes (Fig. 3E) to both, Southern Ocean SST patterns (e.g. Pahnke et al., 2003; Kaiser et al., 2005; Stenni, 2006; Calvo et al., 2007; Lamy et al., 2007; Fig. 3F) and AMOC strength changes (e.g. Böhm et al., 2015 and references therein; Fig. 3B) points to a close coupling of the southern hemisphere climatic development and AMOC variability, and the advection of the resulting thermal anomaly into the tropical intermediate-depth W-Atlantic *via* AAIW. There are indications indeed that the tropical W-Atlantic $IWT_{Mg/Ca}$ temporally lags the AMOC changes by several

hundred years (Fig. 3E), most apparent at the early HS1. Stratigraphic uncertainty, however, hampers any further discussion on temporal phase relationships between deglacial AMOC perturbations, the response of the Southern Ocean, and the possible consequences for the transfer of ocean heat *via* AAIW (see supporting information; Fig. S7). A lagged IWT response in the tropical W-Atlantic resulting from the temperature signal detour *via* the Southern Ocean is nevertheless plausible, but unfortunately not resolvable from the existing sediment records.

In contrast to the εNd record of Core 235, the observed rapid, high-amplitude deglacial changes in $IWT_{Mg/Ca}$ are hence not to result from changes in the water masses feeding AAIW, but rather from a mainly advective transfer of the Southern Ocean thermal anomaly into intermediate depths *via* AAIW formation processes (Fig. 3). A major northward dispersal of Southern Ocean signals *via* intermediate water masses has indeed been suggested before (e.g. Bostock et al., 2004; Rühlemann et al., 2004, c.f. Figure S4; Romahn et al., 2014; Weldeab et al., 2016). Our εNd records imply a gradually decreasing admixture of radiogenic deep waters across the deglaciation at a continuous supply of AAIW from the Southern Ocean. In addition, the intermediate-depth Cd_w data from the same Core 235 *Uvigerina* spp. samples suggest deglacial changes in the AAIW nutrient inventory in the Southern Ocean as a result of changes in deep water upwelling and nutrient injection into the tropical W-Atlantic mainly at the end of HS1 and the YD synchronous with major AMOC reorganizations (Poggemann et al., 2017). We point out that the stability of the ~3-4°C temperature anomaly across thousands of miles from the AAIW-formation sites in the Southern Ocean to the tropical W-Atlantic (Fig. 3) may hence be coincidental in view of the mixing processes. Considering the error bars of approximately +/- 1°C of either reconstruction, a decrease of the initial temperature anomaly in the Southern Ocean on its way north is likely.

Today, AAIW that is present in the tropical W-Atlantic at the location of Core 235 is formed off S-Chile in the SE-Pacific and off S-Argentina in the SW-Atlantic north of the Antarctic Circumpolar Current (Fig. 1) (e.g. Taft 1963; Talley 1996; Boebel et al., 1999; Bostock et al., 2010). The comparison of our Core 235 $IWT_{Mg/Ca}$ record to an $IWT_{Mg/Ca}$ record from Falkland Plateau (Roberts et al., 2016), which is close to the main inflow of today´s AAIW into the Atlantic basin, however, suggests that AAIW formation sites and pathways may have changed considerably over time (Fig. 3E). The Roberts et al. (2016) water-density record derived from their combined $IWT_{Mg/Ca}$ and $\delta^{18}O_{seawater}$ calculations implies that during the LGM the intermediate water mass at Falkland Plateau was rather analogous to modern Antarctic Surface Water (AASW), suggesting that the source location of intermediate water was strongly influenced by sea ice and seasonal sea-ice meltwater. Modern intermediate water at Falkland Plateau, instead, is strongly influenced by a modified component of upwelled CPDW. Only during 6-4 ka BP, Roberts et al. (2016) found evidence for AAIW presence at their core location on Falkland Plateau. As their Core GC528 and our Tobago Basin Core 235 $IWT_{Mg/Ca}$ records converge at ~6 ka BP at ~4°C (showing both resembling $IWT_{Mg/Ca}$ amplitudes downcore; Fig. 3E), we argue that only since then both intermediate sites were affected by the same water mass, namely AAIW. This observation is compatible with our notion that increased Southern Ocean surface warmth was subducted to intermediate depths and transported northward *via* the AAIW as direct response to both major AMOC perturbations and the related heat accumulation in the southern hemisphere.

The downward heat transfer from the surface Southern Ocean during wintertime convection and subsequent northward transport of AAIW at times of prominent AMOC slowdowns or even collapses likely caused the dampening of southern hemisphere atmospheric warming. We hypothesize that the absorption of oceanic heat by AAIW and the subsequent dispersal to the (sub)tropical Atlantic may even have affected Antarctic sea-ice expansion. In particular,

the long phase of storage of Southern Ocean heat by AAIW during the early Holocene (~11 - 7 ka BP) and its subsequent cooling (Fig. 3) may have reduced the intensity of early Holocene warming in the southern hemisphere. We consequently argue that the observed southern hemisphere warming trends during HS1 and the YD would have been even more pronounced if Southern Ocean heat removal *via* AAIW had been absent.

5 Conclusions

Our high-resolution benthic foraminiferal Mg/Ca-based IWT reconstructions from the tropical W-Atlantic indicate pronounced warming of AAIW in the S-Caribbean area during the last deglaciation in close relationship to northern hemisphere abrupt climate-cooling events, consistent with Stocker & Johnson (2003). Combined with εNd reconstructions, upwelling and SST-reconstructions from the Southern Ocean (e.g., Pahnke et al., 2003; Kaiser et al., 2005; Calvo et al., 2007; Lamy et al., 2007; Anderson et al., 2009) and AMOC-strength reconstructions from the N-Atlantic (McManus et al., 2004; Böhm et al., 2015), our data imply a pronounced deglacial heat deprivation from the surface Southern Ocean *via* AAIW formation and the subsequent transfer to intermediate depths. During the deglacial rapid northern hemisphere cooling periods HS1 and the YD, when AMOC considerably weakened or even collapsed, oceanic heat accumulated at the surface Southern Ocean, was subsequently subducted, finally taken up by AAIW, and transferred to the tropical W-Atlantic at intermediate depths. We hypothesize that the rapid deglacial northern climate perturbations directly controlled the AAIW heat budget in the tropical W-Atlantic after a detour *via* the Southern Ocean. As a result the deglacial AAIW heat uptake may have dampened Southern Ocean warming and may therefore have been a crucial player in the climate seesaw mechanisms between the two hemispheres.

Acknowledgments, Samples, and Data

This research was funded by the "Cluster of Excellence – The Future Ocean" Kiel. We would like to thank Katharina Pahnke and Philipp Bönning (University of Oldenburg, Germany) for the Nd isotope measurements. We thank the crew of R/V *Meteor* for their help in the collection of the sediment samples. All data are available online at the Data Publisher for Earth & Environmental Science, PANGAEA: www.pangaea.de. Supporting information associated with this article can be found in the online version (Table SXX).

References

Anderson, R. F., Ali, S., Bradtmiller, L. I., Nielsen, S. H. H., Fleisher, M. Q., Anderson, B. E., & Burckle, L. H. (2009). Wind-driven upwelling in the Southern Ocean and the deglacial rise in atmospheric CO_2. *Science, 323*(5920), 1443-1448.

Barker, S., Greaves, M., & Elderfield, H. (2003). A study of cleaning procedures used for foraminiferal Mg/Ca paleothermometry. *Geochem. Geophys. Geosyst. 4* (9), 1-20. doi:10.1029/2003GC000559

Barker, S., Diz, P., Vautravers, M. J., Pike, J., Knorr, G., Hall, I. R., & Broecker, W. S. (2009). Interhemispheric Atlantic seesaw response during the last deglaciation. *Nature, 457*(7233), 1097-1102. doi:10.1038/nature07770

Barrat, J. A., Keller, F., Amossé, J., Taylor, R. N., Nesbitt, R. W., & Hirata, T. (1996). Determination of rare earth elements in sixteen silicate reference samples by ICP-MS after Tm addition and ion exchange separation. *Geostandards Newsletter, 20*(1), 133-139. doi:10.1111/j.1751-908X.1996.tb00177.x

Boebel, O., Davis, R. E., Ollitrault, M., Peterson, R. G., Richardson, P. L., Schmid, C., & Zenk, W. (1999). The intermediate depth circulation of the western South Atlantic. *Geophysical Research Letters, 26*(21), 3329-3332. doi:10.1029/1999GL002355

Böhm, E., Lippold, J., Gutjahr, M., Frank, M., Blaser, P., Antz, B., et al. (2015). Strong and deep Atlantic meridional overturning circulation during the last glacial cycle. *Nature, 517*(7532), 73-76. doi:10.1038/nature14059

Bostock, H. C., Opdyke, B. N., Gagan, M. K., & Fifield, L. K. (2004). Carbon isotope evidence for changes in Antarctic Intermediate Water circulation and ocean ventilation in

the southwest Pacific during the last deglaciation. *Paleoceanography*, 19(4), PA4013, doi:10.1029/2004PA001047

Bostock, H. C., Opdyke, B. N., & Williams, M. J. M. (2010). Characterising the intermediate depth waters of the Pacific Ocean using $\delta^{13}C$ and other geochemical tracers. *Deep Sea Research Part I: Oceanographic Research Papers, 57*(7), 847-859. doi:https://doi.org/10.1016/j.dsr.2010.04.005

Boyer, T. A., Antonov, J. I., Baranova, O.K., Coleman, C., Garcia, H., Grodsky, A. et al. (2013). World Ocean Database 2013, *NOAA Atlas NESDIS, 72*, S. Levitus, Ed., A. Mishonov, Technical Ed.; Silver Spring, MD, 209 pp..

Bryan, S. P., & Marchitto, T. M. (2008). Mg/Ca–temperature proxy in benthic foraminifera: New calibrations from the Florida Straits and a hypothesis regarding Mg/Li. *Paleoceanography*, 23, PA2220, doi:10.1029/2007PA001553

Broecker, W. S. (1998). Paleocean circulation during the last deglaciation: a bipolar seesaw? *Paleoceanography, 13*(2), 119-121. doi:10.1029/97PA03707

Burke, A., & Robinson, L. F. (2012). The Southern Ocean's role in carbon exchange during the last deglaciation. Science, *335*(6068), 557-561.

Calvo, E., Pelejero, C., De Deckker, P., & Logan, G. A. (2007). Antarctic deglacial pattern in a 30 kyr record of sea surface temperature offshore South Australia. *Geophysical Research Letters, 34*, L13707, doi:10.1029/2007GL029937

Came, R. E., Oppo, D. W., Curry, W. B., & Lynch-Stieglitz, J. (2008). Deglacial variability in the surface return flow of the Atlantic meridional overturning circulation. *Paleoceanography*, 23, PA1217, doi:10.1029/2007PA001450

Crowley, T. J. (1992). North Atlantic deep water cools the Southern Hemisphere. *Paleoceanography, 7*(4), 489-497. doi:10.1029/92PA01058

Denton, G. H., Anderson, R. F., Toggweiler, J. R., Edwards, R. L., Schaefer, J. M., & Putnam, A. E. (2010). The last glacial termination. *Science, 328*(5986), 1652-1656.

Elderfield, H., Yu, J., Anand, P., Kiefer, T., & Nyland, B. (2006). Calibrations for benthic foraminiferal Mg/Ca paleothermometry and the carbonate ion hypothesis. *Earth and Planetary Science Letters, 250*(3), 633-649. doi:https://doi.org/10.1016/j.epsl.2006.07.041

Elderfield, H., Greaves, M., Barker, S., Hall, I. R., Tripati, A., Ferretti, P., et al. (2010). A record of bottom water temperature and seawater $\delta^{18}O$ for the Southern Ocean over the past 440 kyr based on Mg/Ca of benthic foraminiferal *Uvigerina* spp. *Quaternary Science Reviews, 29*(1), 160-169. doi:https://doi.org/10.1016/j.quascirev.2009.07.013

Elmore, A. C., McClymont, E. L., Elderfield, H., Kender, S., Cook, M. R., Leng, M. J., et al. (2015). Antarctic Intermediate Water properties since 400 ka recorded in infaunal (*Uvigerina peregrina*) and epifaunal (*Planulina wuellerstorfi*) benthic foraminifera. *Earth and Planetary Science Letters, 428,* 193-203. doi:https://doi.org/10.1016/j.epsl.2015.07.013

Ferrari, R., Jansen, M. F., Adkins, J. F., Burke, A., Stewart, A. L., & Thompson, A. F. (2014). Antarctic sea ice control on ocean circulation in present and glacial climates. *Proceedings of the National Academy of Sciences, 111*(24), 8753-8758.

Foster, G. L., Vance, D., & Prytulak, J. (2007). No change in the neodymium isotope composition of deep water exported from the North Atlantic on glacial-interglacial time scales. *Geology, 35*(1), 37-40. doi:10.1130/G23204A.1

Freeman, E., Skinner, L. C., Tisserand, A., Dokken, T., Timmermann, A., Menviel, L., & Friedrich, T. (2015). An Atlantic–Pacific ventilation seesaw across the last deglaciation. *Earth and Planetary Science Letters, 424*, 237–244. doi:https://doi.org/10.1016/j.epsl.2015.05.032

Greaves, M., Caillon, N., Rebaubier, H., Bartoli, G., Bohaty, S., Cacho, I., et al. (2008). Interlaboratory comparison study of calibration standards for foraminiferal Mg/Ca thermometry. *Geochemistry, Geophysics, Geosystems,* 9, Q08010, doi:10.1029/2008GC001974

Grubbs (1950). Sample Criteria for Testing Outlying Observations. *The Annals of Mathematical Statistics*, *21*(1), 27–58, doi:10.1214/aoms/1177729885

Grubbs (1969). Procedures for Detecting Outlying Observations in Samples. *Technometrics, 11*(1), 1–21, doi:10.2307/1266761

Gu, S., Liu, Z., Zhang, J., Rempfer, J., Joos, F., & Oppo, D. W. (2017). Coherent response of Antarctic Intermediate Water and Atlantic Meridional Overturning during the last deglaciation: Reconciling contrasting neodymium isotope reconstructions from the tropical Atlantic. *Paleoceanography, 32*. 1036-1053. doi:10.1002/2017PA003092

Gutjahr, M., Frank, M., Stirling, C. H., Keigwin, L. D., & Halliday, A. N. (2008). Tracing the Nd isotope evolution of North Atlantic deep and intermediate waters in the Western North Atlantic since the Last Glacial Maximum from Blake Ridge sediments. *Earth and Planetary Science Letters, 266*(1), 61-77. doi:10.1016/j.epsl.2007.10.037

Hansen, J., Sato, M., Hearty, P., Ruedy, R., Kelley, M., Masson-Delmotte, V., et al. (2016). Ice melt, sea level rise and superstorms: Evidence from paleoclimate data, climate modeling, and modern observations that 2 C global warming could be dangerous." *Atmospheric Chemistry and Physics, 16*(6), 3761-3812. doi:10.5194/acp-16-3761-2016

Howe, J. N. W., Piotrowski, A. M., Oppo, D. W., Huang, K.-F., Mulitza, S., Chiessi, C. M., & Blusztajn, J. (2016). Antarctic intermediate water circulation in the South Atlantic over the past 25,000 years. *Paleoceanography, 31*(10), 1302-1314. doi:10.1002/2016PA002975

Huang, K.-F., Oppo, D. W., & Curry, W. B. (2014). Decreased influence of Antarctic intermediate water in the tropical Atlantic during North Atlantic cold events. *Earth and Planetary Science Letters, 389*, 200-208. doi:https://doi.org/10.1016/j.epsl.2013.12.037

Hunter (2007). Matplotlib: A 2D Graphics Environment. *Computing in Science & Engineering, **9***, 90-95, doi:10.1109/mcse.2007.55

Jeandel (1993). Concentration and isotopic composition of Nd in the South Atlantic Ocean. *Earth and Planetary Science Letters, 117*(3), 581-591.

Kaiser, J., Lamy, F., & Hebbeln, D. (2005). A 70-kyr sea surface temperature record off southern Chile (Ocean Drilling Program Site 1233). *Paleoceanography*, 20, PA4009, doi:10.1029/2005PA001146

Kiefer, T., McCave, I. N., & Elderfield, H. (2006). Antarctic control on tropical Indian Ocean sea surface temperature and hydrography. *Geophysical Research Letters, 33*, L24612, doi:10.1029/2006GL027097

Lamy, F., Kaiser, J., Arz, H. W., Hebbeln, D., Ninnemann, U., Timm, O., et al. (2007). Modulation of the bipolar seesaw in the Southeast Pacific during Termination 1. *Earth and Planetary Science Letters, 259*(3), 400-413. doi:https://doi.org/10.1016/j.epsl.2007.04.040

Landais, A., Masson-Delmotte, V., Stenni, B., Selmo, E., Roche, D. M., Roche, V. A. P., et al. (2015). A review of the bipolar see–saw from synchronized and high resolution ice core water stable isotope records from Greenland and East Antarctica. *Quaternary Science Reviews, 114*, 18-32. doi:https://doi.org/10.1016/j.quascirev.2015.01.031

Lea, D. W., Martin, P. A., Pak, D. K., & Spero, H. J. (2002). Reconstructing a 350 ky history of sea level using planktonic Mg/Ca and oxygen isotope records from a Cocos Ridge core. *Quaternary Science Reviews, 21*, 283–293, doi:10.1016/S0277-3791(01)00081-6

Le Fèvre, B., & Pin, C. (2005). A straightforward separation scheme for concomitant Lu-Hf and Sm-Nd isotope ratio and isotope dilution analysis. *Analytica Chimica Acta, 543*(1-2), 209-221. doi:https://doi.org/10.1016/j.aca.2005.04.044

Lynch-Stieglitz, J., Fairbanks, R. G., & Charles, C. D. (1994). Glacial-interglacial history of Antarctic Intermediate Water: relative strengths of Antarctic versus Indian Ocean sources. *Paleoceanography, 9*(1), 7-29. doi:10.1029/93PA02446

Marchitto, T. M., & Broecker, W. S. (2006). Deep water mass geometry in the glacial Atlantic Ocean: A review of constraints from the paleonutrient proxy Cd/Ca. *Geochemistry, Geophysics, Geosystems*, Q12003, doi:10.1029/2006GC001323

Martin, P. A., Lea, D. W., Rosenthal, Y., Shackleton, N. J., Sarnthein, M., & Papenfuss, T. (2002). Quaternary deep sea temperature histories derived from benthic foraminiferal Mg/Ca. *Earth and Planetary Science Letters, 198*(1), 193-209. doi:https://doi.org/10.1016/S0012-821X(02)00472-7

Mawji, E., Schlitzer, R., Dodas, E. M., Abadie, C., Abouchami, W., Anderson, R. F., et al. (2015). The GEOTRACES Intermediate Data Product 2014, *Marine Chemistry*, http://dx.doi.org/10.1016/j.marchem.2015.04.005

McManus, J. F., Francois, R., Gherardi, J. M., Keigwin, L. D., & Brown-Leger, S. (2004). Collapse and rapid resumption of Atlantic meridional circulation linked to deglacial climate changes. *Nature, 428*(6985), 834-837. doi:10.1038/nature02494

Molina-Kescher, M., Frank, M., & Hathorne, E. (2014). South Pacific dissolved Nd isotope compositions and rare earth element distributions: water mass mixing versus biogeochemical cycling. *Geochimica et Cosmochimica Acta, 127*, 171-189. doi:10.1016/j.gca.2013.11.038

Naidu, P. D., & Govil, P. (2010). New evidence on the sequence of deglacial warming in the tropical Indian Ocean. *Journal of Quaternary Science, 25*(7), 1138-1143. doi:doi:10.1002/jqs.1392

NGRIP Dating Group (2006). Greenland Ice Core Chronology 2005 (GICC05). *IGBP PAGES/World Data Center for Paleoclimatology. Data Contribution Series # 2006-118*, NOAA/NCDC Paleoclimatology Program, Boulder CO, USA.

Ninnemann, U. S., & Charles, C. D. (1997). Regional differences in Quaternary Subantarctic nutrient cycling: Link to intermediate and deep water ventilation. *Paleoceanography, 12*(4), 560-567. doi:10.1029/97pa01032

Oliphant, T.E. (2006). A guide to NumPy, USA. Trelgol Publishing. http: //www.trelgol.com

Osborne, A. H., Haley, B. A., Hathorne, E. C., Flögel, S., & Frank, M. (2014). Neodymium isotopes and concentrations in Caribbean seawater: Tracing water mass mixing and continental input in a semi-enclosed ocean basin. *Earth and Planetary Science Letters, 406*, 174-186. doi:10.1016/j.epsl.2014.09.011

Pahnke, K., Zahn, R., Elderfield, H., & Schulz, M. (2003). 340,000-Year Centennial-Scale Marine Record of Southern Hemisphere Climatic Oscillation. *Science, 301*(5635), 948-952. doi: 10.1126/science.1084451

Pahnke, K., Goldstein, S. L., & Hemming, S. R. (2008). Abrupt changes in Antarctic Intermediate Water circulation over the past 25,000 years. *Nature Geoscience, 1*(12), 870-874. doi:10.1038/ngeo360

Parker, A. O., Schmidt, M. W., & Chang, P. (2015). Tropical North Atlantic subsurface warming events as a fingerprint for AMOC variability during Marine Isotope Stage 3. *Paleoceanography, 30*(11), 1425-1436 . doi:10.1002/2015pa002832

Piepgras, D. J., & Wasserburg, G. J. (1980). Neodymium isotopic variations in seawater. *Earth and Planetary Science Letters, 50*(1), 128-138. doi:https://doi.org/10.1016/0012-821X(80)90124-7

Piepgras, D. J., & Wasserburg, G. J. (1987). Rare earth element transport in the western North Atlantic inferred from Nd isotopic observations. *Geochimica et Cosmochimica Acta, 51*(5), 1257-1271. doi:https://doi.org/10.1016/0016-7037(87)90217-1

Piepgras, D. J., & Jacobsen, S. B. (1988). The isotopic composition of neodymium in the North Pacific. *Geochimica et Cosmochimica Acta, 52*(6), 1373-1381. doi:https://doi.org/10.1016/0016-7037(88)90208-6

Piola, A.R., Georgi, D. T. (1982). Circumpolar properties of Antarctic intermediate water and Subantarctic Mode Water. *Deep Sea Research Part A. Oceanographic Research Papers, 29*(6A), 687-711.

Piotrowski, A. M., Galy, A., Nicholl, J. A. L., Roberts, N., Wilson, D. J., Clegg, J. A., & Yu, J. (2012). Reconstructing deglacial North and South Atlantic deep water sourcing using foraminiferal Nd isotopes. *Earth and Planetary Science Letters, 357*, 289-297. doi:10.1016/j.epsl.2012.09.036

Poggemann, D.-W., Hathorne, E. C., Nürnberg, D., Frank, M., Bruhn, I., Reißig, S., & Bahr, A. (2017). Rapid deglacial injection of nutrients into the tropical Atlantic *via* Antarctic Intermediate Water. *Earth and Planetary Science Letters, 463*, 118-126. doi:10.1016/j.epsl.2017.01.030

Roberts, N. L., Piotrowski, A. M., McManus, J. F., & Keigwin, L. D. (2010). Synchronous deglacial overturning and water mass source changes. *Science, 327*(5961), 75-78. doi:10.1126/science.1178068

Roberts, N. L., Piotrowski, A. M., Elderfield, H., Eglinton, T. I., & Lomas, M. W. (2012). Rare earth element association with foraminifera. *Geochimica et Cosmochimica Acta, 94*, 57-71. doi:10.1016/j.gca.2012.07.00

Roberts, J., Gottschalk, J., Skinner, L. C., Peck, V. L., Kender, S., Elderfield, H., Waelbroeck, C., Vázquez Riveiros, N., Hodell, D. A. (2016). Evolution of South Atlantic density and chemical stratification across the last deglaciation. *PNAS, 113*(3), 514-519.

Romahn, S., Mackensen, A., Groeneveld, J., & Pätzold, J. (2014). Deglacial intermediate water reorganization: new evidence from the Indian Ocean. *Climate of the Past, 10*(1), 293-303. doi:10.5194/cp-10-293-2014

Rühlemann, C., Mulitza, S., Müller, P. J., Wefer, G., & Zahn, R. (1999). Warming of the tropical Atlantic Ocean and slowdown of thermohaline circulation during the last deglaciation. *Nature, 402*(6761), 511-514. doi:10.1038/990069

Rühlemann, C., Mulitza, S., Lohmann, G., Paul, A., Prange, M., & Wefer, G. (2004). Intermediate depth warming in the tropical Atlantic related to weakened thermohaline circulation: Combining paleoclimate data and modeling results for the last deglaciation. *Paleoceanography*, 19, PA1025, doi:10.1029/2003PA000948

Schlitzer, R. (2015). Ocean Data View, http://odv.awi.de

Schmidt, M. W., Chang, P., Hertzberg, J. E., Them, T. R., 2nd, Ji, L., & Otto-Bliesner, B. L. (2012). Impact of abrupt deglacial climate change on tropical Atlantic subsurface temperatures. *Proceedings of the National Academy of Sciences, 109*(36), 14348-14352. doi:10.1073/pnas.1207806109

Schmidt, M. W., Chang, P., Parker, A. O., Ji, L., & He, F. (2017). Deglacial Tropical Atlantic subsurface warming links ocean circulation variability to the West African Monsoon. *Scientific Reports, 7*, 15390, doi:10.1038/s41598-017-15637-6

Sortor, R. N., & Lund, D. C. (2011). No evidence for a deglacial intermediate water $\Delta^{14}C$ anomaly in the SW Atlantic. *Earth and Planetary Science Letters, 310*, 65–72, doi:10.1016/j.epsl. 2011.07.017

Spero, H. J., & Lea, D. W. (2002). The cause of carbon isotope minimum events on glacial terminations. *Science, 296*(5567), 522-525.

Stenni, B. (2006). EPICA Dome C Stable Isotope Data to 44.8 Kyr BP. *IGBP PAGES/World Data Center for Paleoclimatology Data Contribution Series # 2006-112),* NOAA/NCDC Paleoclimatology Program, Boulder CO, USA.

Stenni, B., Buiron, D., Frezzotti, M., Albani, S., Barbante, C., Bard, E., et al. (2011). Expression of the bipolar see-saw in Antarctic climate records during the last deglaciation. *Nature Geoscience, 4*(1), 46-49. doi:10.1038/ngeo1026

Stichel, T., Frank, M., Rickli, J., & Haley, B. A. (2012). The hafnium and neodymium isotope composition of seawater in the Atlantic sector of the Southern Ocean. *Earth and Planetary Science Letters 317*, 282-294. doi:10.1016/j.epsl.2011.11.025

Stocker, T. F. (1998). The seesaw effect. *Science, 282*(5386), 61-62.

Stocker, T. F., & Johnsen, S. J. (2003). A minimum thermodynamic model for the bipolar seesaw. *Paleoceanography*, 18,(4), 1087, doi:10.1029/2003PA000920

Taft, B. A. (1963). Distribution of salinity and dissolved oxygen on surfaces of uniform potential specific volume in the South Atlantic, South Pacific, and Indian Oceans. *Journal of Marine Research, 21*(2), 129-141.

Talley, L. D. (1996). Antarctic intermediate water in the South Atlantic. The South Atlantic. Springer Berlin Heidelberg, 219-238.

Talley, L. D. (2013). Closure of the global overturning circulation through the Indian, Pacific, and Southern Oceans: Schematics and transports. *Oceanography, 26*(1), 80-97.

Tanaka, T., Togashi, S., Kamioka, H., Amakawa, H., Kagami, H., Hamamoto, T., et al. (2000). JNdi-1: a neodymium isotopic reference in consistency with LaJolla neodymium. *Chemical Geology, 168*, 279-281. doi:https://doi.org/10.1016/S0009-2541(00)00198-4

Them, T. R., Schmidt, M. W., & Lynch-Stieglitz, J. (2015). Millennial-scale tropical atmospheric and Atlantic Ocean circulation change from the Last Glacial Maximum and Marine Isotope Stage 3. *Earth and Planetary Science Letters, 427*, 47-56. doi:10.1016/j.epsl.2015.06.062

Toggweiler, J. R., & Lea, D. W. (2010). Temperature differences between the hemispheres and ice age climate variability. *Paleoceanography*, 25, PA2212, doi:10.1029/2009PA001758

Valley, S., Lynch-Stieglitz, J., & Marchitto, T. M. (2017). Timing of deglacial AMOC variability from a high-resolution seawater cadmium reconstruction. *Paleoceanography, 32*, 1195-1203. doi:10.1002/2017pa003099

van de Flierdt, T., Robinson, L. F., Adkins, J. F., Hemming, S. R., & Goldstein, S. L. (2006). Temporal stability of the neodymium isotope signature of the Holocene to glacial North Atlantic. *Paleoceanography*, 21, PA4102, doi:10.1029/2006PA001294

van de Flierdt, T., Griffiths, A. M., Lambelet, M., Little, S. H., Stichel, T., & Wilson, D. J. (2016). Neodymium in the oceans: a global database, a regional comparison and implications for palaeoceanographic research. *Philosophical Transactions of the Royal Society A, 374(2081*). doi:10.1098/rsta.2015.0293

Vellinga, M., Wood, R.A. (2002). Global climatic impacts of a collapse of the Atlantic thermohaline circulation. *Climatic change, 54*(3), 251-267.

Vidal, V. M. V., Vidal, F. V., Hernández, A. F., Meza, E., & Zambrano, L. (1994). Winter water mass distributions in the Gulf of Mexico affected by a colliding anticyclonic ring. *Journal of Oceanography, 50*, 559-588. doi:10.1007/bf02235424

Weldeab, S., Friedrich, T., Timmermann, A., & Schneider, R. R. (2016). Strong middepth warming and weak radiocarbon imprints in the equatorial Atlantic during Heinrich 1 and Younger Dryas. *Paleoceanography, 31*, 1070-1082, https://doi.org/10.1002/2016PA002957

Xie, R. C., Marcantonio, F., & Schmidt, M. W. (2012). Deglacial variability of Antarctic Intermediate Water penetration into the North Atlantic from authigenic neodymium isotope ratios. *Paleoceanography*, 27, PA3221, doi:10.1029/2012PA002337

Xie, R. C., Marcantonio, F., & Schmidt, M. W. (2014). Reconstruction of intermediate water circulation in the tropical North Atlantic during the past 22,000 years. *Geochimica et Cosmochimica Acta, 140*, 455-467. doi:10.1016/j.gca.2014.05.041

Yu, J., & Elderfield, H. (2008). Mg/Ca in the benthic foraminifera *Cibicidoides wuellerstorfi* and *Cibicidoides mundulus*: Temperature versus carbonate ion saturation. *Earth and Planetary Science Letters, 276*(1-2), 129-139. doi:10.1016/j.epsl.2008.09.015

Zahn, R., & Stüber, A. (2002). Suborbital intermediate water variability inferred from paired benthic foraminiferal Cd/Ca and $\delta^{13}C$ in the tropical West Atlantic and linking with North

Atlantic climates. *Earth and Planetary Science Letters*, *200*(1), 191-205.
doi:https://doi.org/10.1016/S0012-821X(02)00613-1

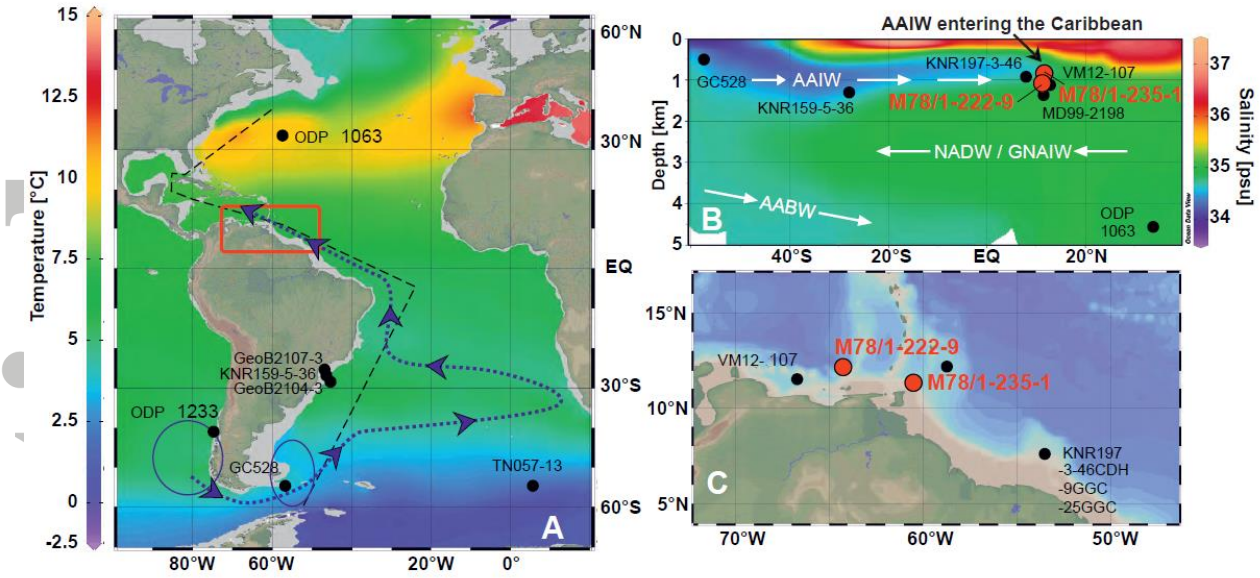

Figure 1. Overview of intermediate water masses in the Atlantic Ocean showing core locations studied here (red) and reference sites (black). **A)** Annual IWT distribution in the Atlantic at 850 m water depth (data from World Ocean Atlas, WOA2013; Boyer et al., 2013). The major pathway of AAIW from its main formation sites (blue ellipses) in the Southern Ocean into the tropical W-Atlantic is marked by the blue dashed line. The study area is indicated by the red square enlarged in C. Black dashed line marks salinity section displayed in B. **B)** Vertical salinity profile (data from WOA2013; Boyer et al., 2013) with locations of proxy records placed at the corresponding water depths (red = this study; black = reference records). Major deep and intermediate water masses are indicated, differentiated by their salinities (AAIW = Antarctic Intermediate Water; NADW = North Atlantic Deep Water; GNAIW = Glacial North Atlantic Intermediate Water; AABW = Antarctic Bottom Water). **C)** Bathymetric chart of the tropical W-Atlantic with locations of the sediment cores (red = this study; black = reference records: ODP1063 - Böhm et al., 2015; ODP1233 - Kaiser et al., 2005 and Lamy et al., 2007; GC528 – Roberts et al., 2016; VM12-107 - Schmidt et al., 2012 and Xie et al., 2014; KNR159-5-36, GeoB2107-3, GeoB2104-3 - Pahnke et al., 2008; Howe et al., 2016; KNR197-3-46CDH, -9GGC, -25GGC – Huang et al., 2014; TN057-13 - Anderson et al., 2009; MD99-2198- Pahnke et al., 2008). Figures created using Ocean Data View (Schlitzer, 2015).

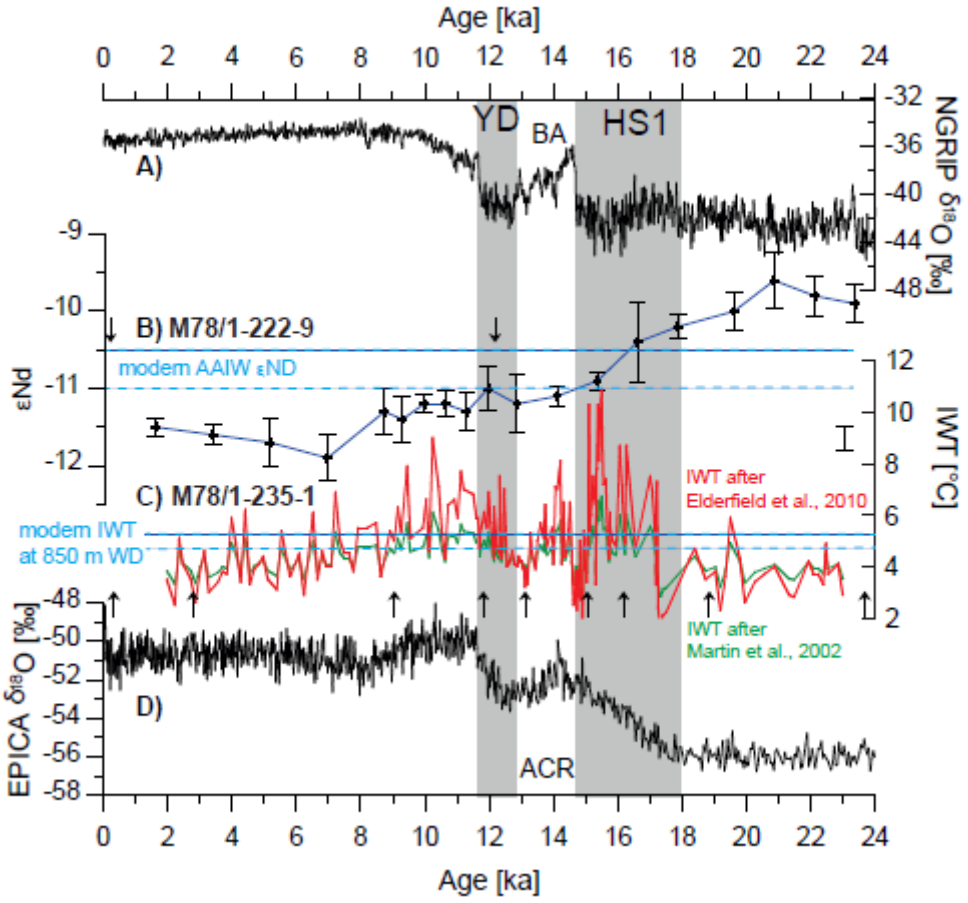

Figure 2. Intermediate water mass evolution in the tropical W-Atlantic during glacial/interglacial change. **A)** Oxygen isotope ($\delta^{18}O$) record of the Greenland NGRIP ice core (NGRIP Dating Group, 2006) as reference for northern hemisphere climate change. **B)** εNd signature of unclean planktonic foraminifera from Tobago Basin (Core 222; 1018 m water depth; this study) reflecting intermediate water mass variability. The modern AAIW εNd signature from the respective water depth close to the core location is indicated by dashed blue lines (Osborne et al., 2014). Vertical bars indicate 2σ-error. **C)** $IWT_{Mg/Ca}$ records based on $Mg/Ca_{Uvigerina}$ of Core 235 (852 m water depth; this study; red record = $Mg/Ca_{Uvigerina}$ calibrated according to Elderfield et al., 2010; green record = $Mg/Ca_{Uvigerina}$ calibrated according to Martin et al., 2002). Dashed blue lines indicate modern IWT at 850 m water depth in the S-Caribbean (from WOA2013; Boyer et al., 2013). The 2σ-error in

$IWT_{Mg/Ca}$ of ~1°C is indicated as a red error bar. **D)** Oxygen isotope ($\delta^{18}O$) record of EPICA Dome C (Stenni, 2006) as reference for the southern hemisphere climate variability. HS1 = Heinrich Stadial 1; YD = Younger Dryas Stadial; BA = Bølling-Allerød; ACR = Antarctic Cold Reversal. Black arrows indicate radiocarbon datings for Core 235 (Poggemann et al., 2017) and Core 222 (this study, see supporting information).

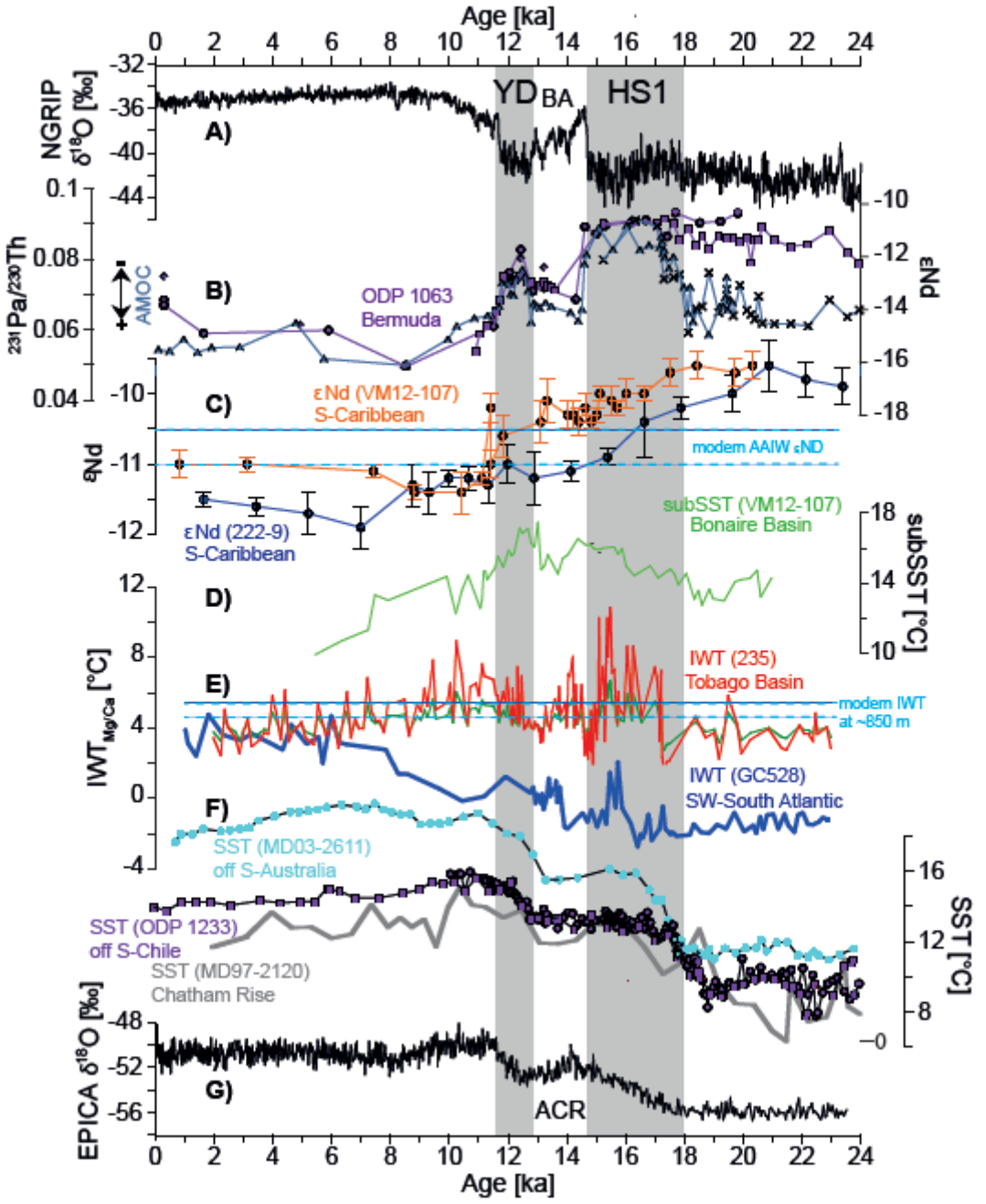

Figure 3. N-Atlantic, tropical W-Atlantic and Southern Ocean proxy records crucial for the interpretation of Atlantic intermediate water dynamics. **A)** Stable oxygen isotope record ($\delta^{18}O$) of the Greenland NGRIP ice core (NGRIP Dating Group, 2006) representing northern hemisphere climate changes. **B)** N-Atlantic overturning strength reconstructed from $^{231}Pa/^{230}Th$ (blue), εNd leachate data of N-Atlantic ODP Site 1063 (purple squares; 4584 m

water depth; Böhm et al., 2015 and references therein), and εNd from uncleaned foraminifers (purple circles; Roberts et al., 2010). **C)** Intermediate water εNd records from the S-Caribbean obtained from sediment cores VM12-107 (orange; 1079 m water depth; Xie et al., 2014) and M78/1-222-9 (blue; 1018 m water depth; this study). Blue stippled lines indicate the modern AAIW εNd signature from the respective water depth close to the core locations (Osborne et al., 2014). **D)** Planktonic foraminiferal Mg/Ca based subsurface temperature ($subSST_{Mg/Ca}$) reconstruction obtained from S-Caribbean Core VM12-107 (green; 1079 m water depth; Schmidt et al., 2012). **E)** $Mg/Ca_{\textit{Uvigerina}}$-based IWT record of Core 235 (this study; 852 m water depth; green record = $Mg/Ca_{\textit{Uvigerina}}$ calibrated according to Martin et al., 2002; red record = $Mg/Ca_{\textit{Uvigerina}}$ calibrated according to Elderfield et al., 2010) in comparison to a SW S-Atlantic $IWT_{Mg/Ca}$ record (solid blue; Core GC528; 598 m water depth; Roberts et al., 2016). Dashed blue lines indicate modern IWT at 850 m water depth in the S-Caribbean (from WOA2013; Boyer et al., 2013). **F)** Alkenone-based sea-surface temperature (SST) reconstructions from the SE-Pacific (purple; ODP Site 1233; 838 m water depth; Kaiser et al., 2005 (squares); Lamy et al., 2007 (dots)) and from offshore S-Australia (cyan; Core MD03-2611; 2420 m water depth; Calvo et al., 2007). The $Mg/Ca_{\textit{G.bulloides}}$-based SST record from Chatham Rise (solid gray; Core MD97-2120; 1210 m water depth; Pahnke et al., 2003) supports the Southern Ocean alkenone records. **G)** Stable oxygen isotope ($\delta^{18}O$) reference record from Antarctica EPICA Dome C (Stenni, 2006) reflecting southern hemisphere climate changes. HS1 = Heinrich Stadial 1; YD = Younger Dryas Stadial; BA = Bølling-Allerød; ACR = Antarctic Cold Reversal.

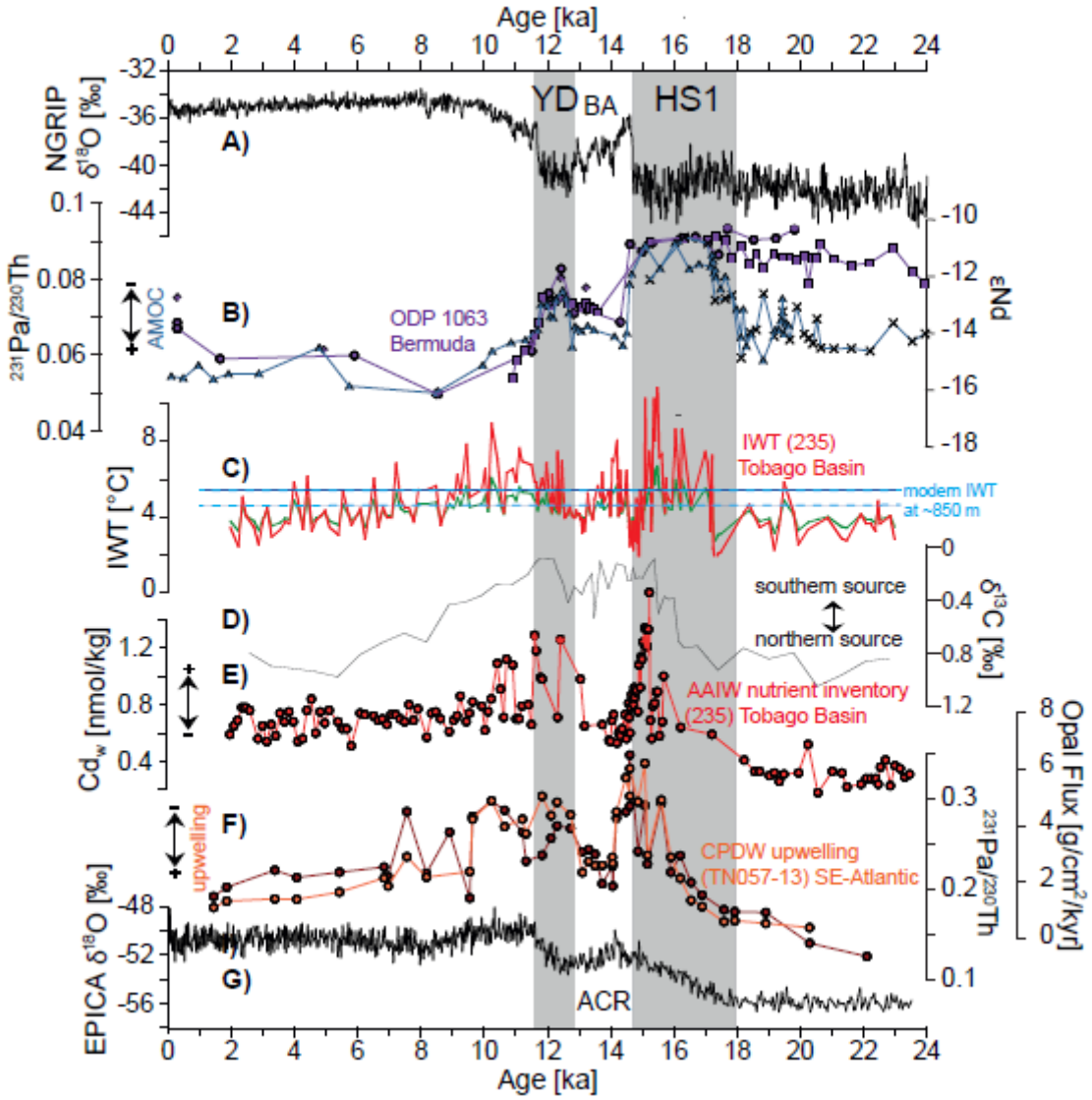

Figure 4. N-Atlantic, tropical W-Atlantic and Southern Ocean proxy records crucial for the interpretation of Atlantic intermediate water dynamics. **A)** Stable oxygen isotope record ($\delta^{18}O$) of the Greenland NGRIP ice core (NGRIP Dating Group, 2006) representing northern hemisphere climate changes. **B)** N-Atlantic overturning strength reconstructed from $^{231}Pa/^{230}Th$ (blue), εNd leachate data of N-Atlantic ODP Site 1063 (purple squares; 4584 m water depth; Böhm et al., 2015 and references therein), and εNd from uncleaned foraminifers (purple circles; Roberts et al., 2010). **C)** $Mg/Ca_{Uvigerina}$-based IWT record of Core 235 (852 m water depth; this study; green record = $Mg/Ca_{Uvigerina}$ calibrated according to Martin et al.,

2002; red record = $Mg/Ca_{Uvigerina}$ calibrated according to Elderfield et al., 2010). Dashed blue lines indicate modern IWT at 850 m water depth in the S-Caribbean (from WOA2013; Boyer et al., 2013). **D)** Benthic $\delta^{13}C$-record (*Uvigerina* spp.) from tropical W-Atlantic Core 235 indicating relative changes in southern *vs.* northern-sourced water masses (Poggemann et al., 2017). **E)** Temporal change in AAIW nutrient inventory (Cd_w) for the tropical W-Atlantic Core 235 based on benthic $Cd/Ca_{Uvigerina}$ ratios (Poggemann et al., 2017). **F)** Record of nutrient-rich CPDW upwelling in the SE-Atlantic based on opal flux (orange) and $^{231}Pa/^{230}Th$ ratios (brown) of S-Atlantic Core TN057-13 (2848 m water depth; Anderson et al., 2009). **G)** Stable oxygen isotope ($\delta^{18}O$) reference record from Antarctica EPICA Dome C (Stenni, 2006) reflecting southern hemisphere climate changes. HS1 = Heinrich Stadial 1; YD = Younger Dryas Stadial; BA = Bølling-Allerød; ACR = Antarctic Cold Reversal.